Evaluation of rhBMP-2 and bone marrow derived stromal cell mediated bone regeneration using transgenic fluorescent protein reporter mice

Shalini V. Gohil[1,2], **Douglas J. Adams**[1], **Peter Maye**[3,4], **David W. Rowe**[3,4], and **Lakshmi S. Nair**[1,2,5,6]

[1]Department of Orthopedic Surgery, University of Connecticut Health Center, Farmington, Connecticut 06032

[2]Institute for Regenerative Engineering, The Raymond Beverly Sackler Center for Biomedical, Biological, Physical and Engineering Sciences, University of Connecticut Health Center, Farmington, Connecticut 06032

[3]Center for Regenerative Medicine and Skeletal Development, Department of Reconstructive Sciences, University of Connecticut Health Center, Farmington, Connecticut 06030

[4]School of Dental Medicine, University of Connecticut Health Center, Farmington, Connecticut 06030

[5]Department of Material Science and Engineering, Institute of Material Science, University of Connecticut, Storrs, Connecticut 06269

[6]Department of Biomedical Engineering, University of Connecticut, Storrs, Connecticut 06269

Abstract

The aim of the study is use of transgenic fluorescent protein reporter mouse models to understand the cellular processes in recombinant human bone morphogenetic protein-2 (rhBMP-2) mediated bone formation. Bilateral parietal calvarial bone defects in Col3.6Topaz transgenic fluorescent osteoblast reporter mouse were used to understand the bone formation in the presence and absence of rhBMP2 and/or Col3.6Cyan bone marrow derived stromal cells (BMSCs), using collagen-hydroxyapatite matrix (Healos) as a biomaterial. The bone regeneration was not confined to the site of BMP-2 implantation and significant bone formation was observed in the neighboring defect site. Osteogenic cellular activity with overlying alizarin complexone staining was observed in both the defects indicating host cell induced mineralization. However, implantation of BMSCs along with rhBMP-2 demonstrated a donor cell derived bone formation. The presence of rhBMP-2 did not support host cell recruitment in the presence of donor cells. This study demonstrates the potential of multiple fluorescent reporters to understand the cellular processes involved in the bone regeneration process using biomaterials, growth factors, and/or stem cells.

INTRODUCTION

Treatment of trauma, disease, and bone resection surgeries and developmental defects pose a major challenge in clinical settings and require the use of various bone regeneration strategies including autografts, allografts, and synthetic bone grafts. Commercially available bone grafts are based on the use of osteoinductive growth factors such as bone morphogenetic proteins (BMPs) delivered using a biocompatible matrix.[1] BMPs, which belong to the transforming growth factor superfamily, are potent inducers of bone formation and simultaneously stimulate migration, proliferation, and differentiation of uncommitted mesenchymal stem cells (MSCs) along the osteogenic lineage.[2] BMP-2 has shown to promote osteoblast differentiation by enabling p300-mediated acetylation of Runx2, as well as significantly upregulate alkaline phosphatase (ALP) activity through the Wnt3a and β-catenin pathway.[3,4]

Bone marrow derived MSCs retain the potency to differentiate into several tissue types including bone, and studies have showed the synergistic effect of MSCs and BMPs for improved bone regeneration.[5,6] A mechanistic model explaining osteoblast differentiation of MSCs suggested crosstalk between BMPs and canonical Wnts that converge on Runx2.[7] Burastero et al.[8] showed improved bone regeneration of critical-size segmental defects in athymic rats using human MSCs (hMSCs) with BMP-7 compared to either hMSCs or BMP-7 alone. Therapeutic potential of multipotent MSCs may also lie in their ability to produce trophic factors that are delivered to the host tissue microenvironment, facilitating the regenerative process.[9] The contribution of host and donor cells in stem cell mediated bone repair/regeneration remains poorly understood. A number of methods, such as polymeric and magnetic nanoparticles, dendrimers, and quantum dots, have been used for *in vitro* and *in vivo* cellular targeting and imaging applications to understand these phenomenons. However, these suffer from drawbacks, such as lack of sensitivity and molecular specificity, and in some cases, cellular toxicity.[1] Transgenic green fluorescent protein (GFP) reporter animal models may provide a unique advantage by providing a functional readout of the cellular response to the regeneration process in presence of growth factors and/or multipotent stem cells.

The properties of the carrier can also modulate the pharmacokinetics and the extent of BMP diffusion to nontargeted tissues, and thus, may significantly affect the clinical outcome.[10] The standard clinical practice for localized BMP delivery involves implantation after physical adsorption on a collagen sponge.[11] However, collagen does not have BMP-binding sites, which leads to rapid diffusion of rhBMP-2 away from the implantation site. This necessitates the use of supraphysiological doses which are associated with clinical complications including soft tissue swelling, inflammation, ectopic or heterotopic bone formation, and osteolysis.[12] Novel biomaterials with higher rhBMP-2 retention as well as *in*

vivo models for assessing the effect of long-range diffusional properties of BMP at the cellular level are, therefore, needed to develop improved rhBMP-2 therapies.

Previously, we reported on the generation of osteoblast fluorescent protein reporter mice containing a 3.6-kilobase DNA fragment (pOBCol3.6) derived from the rat type I collagen (Col1a1) promoter that directs strong expression of fluorescent proteins (Cyan and Topaz) in bone tissues.[13] The generation of spectrally distinct fluorescent protein variants Col3.6Tpz (green) and Col3.6Cyan (blue) allows us to histologically distinguish two different sources of osteoblasts (host and donor) during transplantation experiments. Additionally, a new method of histological analysis was developed for these transgenic reporter mice, which allows preservation of fluorescence in nondecalcified bone, enabling the imaging of osteoblast reporters with mineralization fluorochromes, ALP staining, and tartrate-resistant acid phosphatase (TRAP) staining. Collectively, these histological analyses provide an in-depth characterization of bone repair at the cellular level.

One of our long-term objectives is to develop biomaterials that can serve as localized delivery vehicles for growth factors and cells, either alone or in combination. In the present study, a bilateral calvarial defect model in fluorescent protein reporter mice was used as a tool to follow cellular events on localized cell and/or rhBMP-2 delivery, as a function of time *in vivo*. Healos, a commercially available osteoconductive sponge made of collagen fibers coated with hydroxyapatite was used as the delivery vehicle. The study was divided into two parts. The first part of the study focused on understanding the cellular processes of bone regeneration, following *in vivo* rhBMP-2 delivery, using Col3.6Tpz mice. The second part investigated the role of host and donor cell contribution to bone regeneration in the presence and absence of rhBMP-2. For this, Col3.6cyan mice were used to isolate bone marrow derived stromal cells (BMSCs), which were then transplanted into the recipient Col3.6Tpz mice.

MATERIALS AND METHODS

Materials

Chinese hamster ovary (CHO) cell-derived rhBMP-2 and rhBMP-2 enzyme-linked immunosorbent assay (ELISA) kit were obtained from R&D Systems. Healos (3.5 mm diameter × 0.5 mm thickness) was purchased from DePuy Orthopaedics, Hoechst 33342 was procured from Mol Probes, and ELF®97 phosphatase substrate was purchased from Life Technologies. Fast Red-TR and Naphthol AS-MX Phosphate was obtained from Sigma. Shandon cryomatrix™ was purchased from Thermo Scientific. Mayer's modified hematoxylin was purchased from PolyScientific. All other chemicals used were of reagent or pharmaceutical grade and obtained from Fisher Scientific.

In vitro rhBMP-2 release

Reconstituted rhBMP-2 (2 μg/7 μL PBS) was added dropwise onto Healos (*n* = 4) and incubated for 5 min. The release study was performed by immersing the discs in 400 μL phosphate buffer solution (PBS) at 37°C with constant shaking on a rocker table. At each time point (1, 5, 7, 24, 48, 120, 240, and 360 h), 200 μL of the release medium was removed

and replaced with an equal amount of PBS. The rhBMP-2 released at each time point was quantified using ELISA.

In vivo study design

The institutional animal care committee approved all aspects of the experimental protocol. The following mice were used in this study: CD-1 transgenic mice containing the 3.6-kb fragment of the rat collagen type 1 promoter fused to a topaz-fluorescent protein (Col3.6-Tpz) ($n = 12$); CD-1 transgenic mice containing the 3.6-kb fragment of the rat collagen type 1 promoter fused to a cyan-fluorescent protein (Col3.6-Cyan) ($n = 6$); nontransgenic CD1 mice ($n = 2$). The Col3.6-tpz and Col3.6-Cyan mice were constructed in the laboratory of Dr. David Rowe. The transgenic mice used in this study were generated, bred and maintained at the Center for Laboratory Animal Care of the UConn Health Center. The animals had free access to both sterile water and standard rodent chow *ad libitum*. All the experimental animals were used between 11 and 13 weeks of age with an average weight of 39 ± 6 g. rhBMP-2 (2 μg/7 μL PBS) was added to Healos and incubated for 5 min before implantation [Fig. 1(A)]. Table I shows the details of different samples studied. Bilateral, critical sized, parietal defects were made in the calvaria of Col3.6Tpz transgenic mice followed by the treatments described in Table I ($n = 3$, at 4 and 8 weeks; Supporting Information Fig. S1A). In the first study, the right defects were implanted with Healos soaked in 2 μg of rhBMP-2 dissolved in 7 μL PBS (H+BMP). The left defects were implanted with Healos soaked in 7 μL PBS (H−BMP). In the second study, right defects were implanted with Healos seeded with 1×10^6 BMSCs with 2 μg rhBMP-2 dissolved in PBS (total volume 7 μL), (H+C+BMP) prior to transplantation. The left defects were implanted with Healos seeded with 1×10^6 BMSCs in 7 μL PBS without rhBMP-2 (H+C −BMP).

Surgery details

***In vivo* bone repair using rhBMP-2**—Col3.6Tpz mice were anesthetized with ketamine (135 mg/kg)/xylazine (15 mg/kg) by intraperitoneal injection before transplantation. The head was shaved and the surgical site was cleaned with 75% ethanol. An incision was made just off the sagittal midline to expose the parietal bone. The pericranium was removed, and 3.5 mm defects were made on both sides of nonsuture-associated parietal bone using a trephine drill. After implantation (as described in Table I), the skin was sutured. One day before tissue harvest, mice were injected intraperitoneally with alizarin complexone (AC; 30 mg/kg body weight).[14]

***In vivo* bone repair using rhBMP-2 and donor BMSCs**—Col3.6Cyan mice were used to derive BMSC cultures. Briefly, 2–3-month-old mice were sacrificed by CO_2 asphyxiation followed by cervical dislocation. The epiphyseal growth plates of the femurs and tibias were removed, and the bone marrow was collected by flushing with α-MEM culture medium containing 100 U/mL penicillin, 100 μg/mL streptomycin, and 10% FCS with a 25-gauge needle. Single cell suspensions were prepared by gently mixing the cells with a pipette, followed by filtration through a 70-μm strainer. Cells were centrifuged at $350g$ for 10 min and plated at a density 3×10^6 cells/cm^2. At day 4 of seeding, half of the medium was replaced with fresh α-MEM culture medium. At day 6, complete medium was

replaced with fresh medium. At day 7, the cells were washed with PBS and digested with trypsin/EDTA solution.

The recipient (Col3.6Tpz) mice underwent total body gamma irradiation before transplantation with ^{137}Cs (Nordion Gammacell 40 Irradiator) to overcome immune rejection according to a reported procedure.[15] A dose of 9.0 Gy (900 rad) was used to ablate the bone marrow. Within 24 h after irradiation, the mice received a bone marrow donation from nontransgenic CD1 mice where a volume of 200 μL with 5×10^6 cells was introduced into the retro-orbital sinus. The surgery was performed in the same way as described in section "In vivo bone repair using rhBMP-2". Col3.6Cyan BMSCs (1×10^6) were redispersed in 7 μL PBS with or without 2 μg rhBMP-2 followed by dropwise addition on Healos for implantation (Table I).

Tissue analysis—Samples were harvested after 4 or 8 weeks of surgical implantation. At each time point, the animals were sacrificed by CO_2 asphyxiation followed by cervical dislocation. Calvaria were dissected from the skull, fixed in 10% formalin, and imaged radiographically at 4× magnification (6 s at 26 kVp) using a digital capture X-ray cabinet (Faxitron LX-60). Quantitative new bone formation was analyzed by measuring the relative radio-opacity of host bone and new bone, using ImageJ software (National Institutes of Health, Bethesda, MD). Briefly, the radio-opacity of the defect area and host was measured by ImageJ and the relative radio-opacity was calculated by dividing the defect area radio-opacity with host bone radio-opacity.[16] The extent of radio-opacity was expressed as mean ± standard deviation. Statistical analysis was performed using t-test and p-values less than 0.050 were considered significant.

After 4 days of formalin fixation, the calvaria were transferred into a 30% sucrose solution in PBS, pH 7.4. The tissue was then positioned in Shandon cryomatrix™, frozen on dry ice and stored in airtight plastic bags at −20°C until sectioning. Cryosections (5 μm) through the nondecalcified calvaria were obtained on a Leica CM3050S cryostat (Leica, Wetzlar) using a disposable steel blade (Thermo Scientific) and tape transfer process (Cryofilm type IIC(10), Section-Lab Co. Ltd.; Supporting Information).[17] For brightfield imaging, sections were initially imaged under differential interference contrast (DIC) optics using a MIRAX MIDI slide scanner (Carl Zeiss). Endogenous fluorescence of Col3.6cyan was detected with Cyan Fluorescent Protein (CFP) (blue) filter and Col3.6Tpz with Yellow Fluorescent Protein (YFP) (yellow-green) filter. AC labeling was detected with MCherry filter. This combination of CFP, YFP, MCherry, and DIC enabled visualization of the endogenous fluorescence of the Tpz (recipient) mice and cyan (donor cells) while highlighting the newly formed mineralized layer in the nondecalcified section. The section was then stained for TRAP for which the slides were covered with freshly prepared preincubation solution (112 mM sodium acetate, 76 mM sodium tartrate, and 11 mM sodium nitrite, pH 4.1–4.3) at RT for 10 min. The slide was then drained and covered with the same buffer now containing 60 μM ELF$^®$97 phosphatase substrate followed by UV exposure for about 5 min at room temperature. The reaction was stopped by submerging the slides with three changes of PBS for 10 min with gentle agitation. Slides were cover slipped with 50% glycerin in PBS and imaged with a combination of yellow filter optimized for tetracycline (Chroma Technology Custom HQ409sp, 425dcxr, HQ555/30, set lot C-104285) and YFP filter. Next the cover slip was

removed and the slide was stained for ALP activity. The slide was incubated in the ALP reaction buffer (100 mM Tris, pH 9.5, 50 mM MgCl$_2$, 100 mM NaCl) for 10 min followed by incubation in reaction buffer containing 0.2 mg/mL Fast Red TR and 0.1 mg/m Naphthol AS-MX Phosphate for 5 min. After washing in PBS, the section was covered with 50% glycerol containing 10 μg/mL of Hoechst 33342 and the slide was cover slipped for imaging using a combination of Tomato (red) and 4′,6-diamidino-2-phenylindole (DAPI) filters. This step was followed by decalcification with a 14% EDTA solution and counterstaining with Mayer's hematoxylin followed by brightfield imaging.[18]

RESULTS

In vitro BMP-2 release

Figure 1(B) shows the *in vitro* % cumulative release of rhBMP-2 from Healos at 37°C. A burst release of 7.6% (~153 ng) was observed within the first 4 h of *in vitro* release. No apparent release was observed thereafter. The Healos retained ~92% of the encapsulated rhBMP-2, even after 15 days of incubation in PBS under the *in vitro* release conditions.

Whole tissue analysis

Figure 2 shows (A) the photographs of isolated whole calvaria and (B) X-ray scans of representative samples of each group ($n = 3$). Figure 2(C) shows the photographs and X-ray scans of defect sites implanted with Healos when the neighboring site was not implanted with rhBMP-2 containing scaffold, at 4 and 8 weeks postimplantation. Healos alone was not able to show bone formation, at both the time points. However, on rhBMP-2 implantation (H +BMP) in the left defect, significant bone formation was observed in the neighboring site implanted with Healos alone (H−BMP) [Fig. 2(B1)]. Figure 2(D) shows the relative radio-opacity of the defect site versus host bone. At 4 weeks, a significant increase was observed in the relative radio-opacity in H−BMP and H+BMP groups, compared to Healos. Implantation of BMSCs and rhBMP-2 together (H+C+BMP) resulted in a significant increase in bone formation compared to H+BMP group at 4 weeks [Figs. 2B4 and B2, respectively].

Histological analysis

***In vivo* bone repair using rhBMP-2**—Figure 3 shows representative images of the regeneration sites of H−BMP and H+BMP groups, at 4 weeks post-implantation. Tissue sections were imaged for bone mineral (DIC optics), osteoblasts (Col3.6Tpz expression, green, top left), osteoclasts (TRAP top right; yellow), ALP activity (red) merged with DAPI (white; bottom left), and hematoxylin (bottom right). High magnification images of two areas corresponding to the surface (a and c) and the middle region (b and d) of the regenerated tissue are also shown. Supporting Information Figure S1B shows a pictorial presentation explaining the use of GFP reporter expression and histological staining to identify the cellular response during bone formation. At 4 weeks, the DIC image of H+BMP and H−BMP groups showed presence of newly formed trabecular bone-like structure (indicated by #, Fig. 3, DIC). The newly regenerated bone surface showed the presence of a periosteum-like tissue consisted of weakly GFP positive fibroblastic cells (indicated by *). The middle region of the regenerated tissue showed osteocytes embedded in the newly

formed bone. Imaging of Col3.6Tpz reporter expression showed GFP positive osteoblasts on the bone surface next to the mineralizing AC label (thin red line), and GFP positive osteocytes embedded in newly formed bone. The ALP-stained sections also showed high ALP activity in the Col3.6Tpz positive osteoblasts in both H+BMP and H−BMP groups (Fig. 3, ALP). Areas of nonmineralized marrow were also observed around trabecular bone (indicated by α). These areas did not show any ALP activity. Osteoblast nuclei could be observed buried in ALP positive red fluorescence. Hematoxylin staining also showed trabecular-like bone with embedded osteocyte nuclei and marrow cells with very few adipocytes (Fig. 3, hematoxylin). The TRAP staining of the regenerated area showed high osteoclast activity at 4 weeks in both H+BMP and H−BMP groups indicating active bone remodeling (Fig. 3, TRAP).

Figure 4 shows representative images of the repair site H−BMP and H+BMP groups, at 8 weeks post-implantation. The H+BMP group showed remodeled bone containing mineralized bony areas arising from host Col3.6Tpz positive osteoblasts next to a mineralizing AC label (Fig. 4, DIC c&d). The potent osteogenic activity in the H+BMP group is further confirmed by the ALP staining (Fig. 4, ALP, c&d). Areas of ALP positive cells lining the mineralized trabecular-like bone with embedded osteocytes could be seen surrounding ALP negative, nonmineralized, cell-rich marrow containing very few adipocytes (indicated by circle; Fig. 4, ALP c&d). The observation was supported by the hematoxylin staining showing trabecular-like bone (indicated by #) with a cellular-rich bone marrow (indicated by a; Fig. 4, hematoxylin c&d).

The DIC images of the H−BMP group conversely showed a decrease in trabecular bone in the defect area compared to 4 weeks as shown in X-ray images, indicating the possible inability to maintain the newly formed bone. This is corroborated by a decrease in ALP positive cells in H−BMP groups both on the surface and the middle region of the defect area at 8 weeks, postimplantation (Fig. 4, ALP a&b). Hematoxylin staining confirmed the presence of fibrous tissue (indicated by $) in H−BMP treatment (Fig. 4, hematoxylin b). Similar to 4 weeks, the H−BMP defect site (Fig. 4, TRAP a&b) showed high osteoclast activity in all replicates. The H+BMP group conversely showed reduced osteoclast activity at 8 weeks compared to 4 weeks (Fig. 4, TRAP c&d).

***In vivo* bone repair using rhBMP-2 and donor BMSCs—**Figure 5 shows the representative images of DIC-, TRAP-, ALP-, and hematoxylin-stained sections of H+C+BMP and H+C−BMP treatments, at 4 weeks post-implantation. The DIC sections showed the presence of early woven bone with a disorganized mineralized matrix (indicated by ^), confirmed by diffuse AC labeling as well as ALP staining, throughout the defect area. The periosteum-like tissue composed of weakly positive host-derived fibroblastic cells could be observed at the outer region of defect area (indicated by *). Col3.6Cyan donor derived osteoblasts were seen predominantly within the defect area along with few Col3.6Tpz cells. Hematoxylin staining further confirmed the presence of disorganized mineralized matrix with marrow-like tissue, in both H+C+BMP and H+C−BMP groups (Fig. 5, hematoxylin). No differences were observed in the left and right defects, with or without rhBMP-2. However, osteoclast activity was found to be highly variable within the triplicate samples for both H+C+BMP and H+C−BMP groups at 4 weeks (Fig. 5, TRAP c).

Figure 6 shows the representative images of DIC-, TRAP-, ALP-, and hematoxylin-stained sections of H+C−BMP and H+C+BMP treatments, at 8 weeks post-implantation. The histological evaluation at 8 weeks (Fig. 6, DIC) showed that the mineralized early woven bone observed at 4 weeks disappeared and was replaced by a uniform, compact, cortical-type bone (indicated by @), with a central nonmineralized marrow cavity (indicated by α). The cortical-type bone of both H+C+BMP and H+C−BMP groups was mostly composed of donor Col3.6Cyan positive cells and only a very few host-derived Col3.6Tpz cells were observed (Fig. 6, DIC). The outer periosteum-like tissue was composed of weakly positive host-derived Col3.6Tpz cells (Fig. 6, DIC, *). The presence of osteogenic cells in the cortical-type bone in both H+C+BMP and H+C−BMP groups was further confirmed by ALP staining. As shown in the figure, the middle area of the cortical-type bone is completely filled with marrow-like ALP-negative tissue (Fig. 6, ALP). This is further confirmed by hematoxylin staining indicating the presence of marrow containing few adipocytes (denoted by circle), surrounded by mature cortical-type bone embedding osteocytes (Fig. 6, hematoxylin). Minimal osteoclast activity was observed in both H+C−BMP and H+C+BMP treatments at 8 weeks, unlike H−BMP treatment (Fig. 6, TRAP).

DISCUSSION

The aim of this study was to use fluorescent protein reporter mice as a novel tool, to follow the cellular events involved in bone regeneration on rhBMP-2 treatment with and without BMSCs and test the ability of biomaterial to confine the bone formation at the defect site. Localization of rhBMP-2 and cells at the healing site is crucial to support successful bone regeneration as well as to prevent ectopic bone formation. Bilateral calvarial defect model has been widely used to study bone formation in the presence of cell/growth factor loaded scaffolds.[19–21] We have previously used this model to evaluate the differences in behavior of calvarial derived osteoblasts and BMSCs in supporting bone regeneration demonstrating the efficacy of the model.[16,22] Laterally performed craniotomies have the advantage of allowing paired design and minimized morbidity.[23] The proximity of the bilateral defects requires the localization of cells and growth factors at the respective defect sites and therefore may serve as a suitable model to evaluate long-range, off-target effects of BMP-2 released from the implanted scaffold. When combined with the use of transgenic mice, the model could help in studying the cellular aspects of BMP-mediated bone healing at the implantation site and the neighboring defect site, in the presence and absence of transplanted cells.

The optimal dose and release kinetics of rhBMP-2 for localized bone regeneration is not well understood. Even though rhBMP-2 has been found to be effective *in vitro* at nanogram range, supraphysiological doses are necessary for *in vivo* bone formation.[24,25] Freilich et al.[26] tested titanium implants loaded with 20 µg rhBMP-2/scaffold in a mouse calvarial model and observed large outgrowths, after 3 weeks. Rahman et al.[27] showed only a 55% increase in bone formation compared to control after 6 weeks of implantation with poly(lactic-co-glycolic) acid/polyethylene glycol scaffolds loaded with 1 µg BMP-2 in a mouse bilateral calvarial bone defect model. Therefore, a dose of 2 µg/defect was used in the present study to achieve complete bone formation by 4 weeks to follow the cellular response using fluorescent reporter cells.

The release kinetics of rhBMP-2 from Healos may depend on several factors, such as the diffusion of the protein through the collagen-hydroxyapatite matrix, interaction of the protein with the matrix and the degradation rate of the matrix. Xie et al.[28] investigated the role of hydroxyapatite nanoparticles as controlled release carrier of BMP-2 and showed that BMP adsorption on these nanoparticles could be as high as 70 μg/mg. In the present study, Healos showed high rhBMP-2 retention *in vitro* and the less than 10% rhBMP-2 release is presumably due to the strong binding of the protein by the hydroxyapatite coating on Healos. However, significant bone formation was observed *in vivo* at both the rhBMP-2 implantation site and the neighboring site. Under *in vivo* conditions, a much higher release of rhBMP-2 is possible due to the enzymatic degradation of the collagen matrix. Use of radiolabeled rhBMP-2 may provide a better understanding of the *in vivo* concentration of rhBMP-2 at the respective defect sites and needs to be investigated further. Additionally, systemic effects of rhBMP-2 on circulating progenitors may also modulate the bone formation by inducing circulating progenitor cell homing.[29,30] Several biomaterial-based approaches are currently underway to minimize the side effects by localizing rhBMP-2 at the site of implantation and reducing rhBMP-2 dose. For instance, Mariner et al.[31] reported the possibility of reducing the therapeutic range of rhBMP-2 by 10-fold, using a peptide functionalized poly(ethylene glycol) hydrogel. Martino et al.[32] used a fibrin-based matrix and showed significant bone formation with a low BMP-2 dose (100 ng) when used in the presence of 2 μM multifunctional fibronectin domains (FN III9*-10/12–14) and PDGF-BB, indicating the possibility of engineering biomaterials to localize rhBMP-2.

The Col3.6 promoter regulates expression of a fluorescent protein that is detected at a lower level in preosteoblastic cells, which become fully differentiated bone cells.[18] When osteoblastic differentiation occurs, the fluorescent protein expression is upregulated. Actively mineralizing osteoblasts thus show a strong GFP expression making identification of the source of bone forming cells possible. Staining techniques (ALP and TRAP) and fluorochromes (AC) further help in identifying osteoblasts and osteoclasts in the regenerating tissue (Supporting Information Fig. S1B). Since Col3.6 osteoblast reporter mice are specific reporters for active bone formation, they can be used to understand the response of osteoprogenitor cells to rhBMP-2 treatment and also for interpreting results from transplantation experiments.

The fluorescent protein reporter mice help to decipher host osteoblast and osteoclast activation and spatial distribution of osteoblasts, mineralizing osteoblasts, osteoclasts, and periosteal fibroblasts, at the site of rhBMP-2 loaded scaffolds as well as in the neighboring defect sites.[13,16,18,22] The relative radio-opacity (Fig. 2D) showed significant bone formation in both H−BMP and H+BMP groups compared to Healos at 4 weeks. Both the groups showed the presence of trabecular-like bone, with bone surface labeled red (AC), with overlaying Col3.6 green osteoblast cells. At 8 weeks, the H+BMP groups maintained the trabecular bone structure; however, the H−BMP group showed signs of some bone loss. No differences in relative radio-opacity were observed in H+BMP group at 4 and 8 weeks (p = 0.144). In H-BMP group, even though the relative radio-opacity at 4 weeks (0.95 ± 0.34) was greater than that observed at 8 weeks (0.47 ± 0.20), the difference was not statistically significant (p = 0.055). rhBMP-2 not only promotes osteogenic differentiation of MSCs but also induces osteoclastogenesis and osteoclast stimulation in a dose- and time-dependent

manner.[33,34] No visual differences in osteoclast activity were observed in H+BMP and H−BMP groups at 4 weeks as evidenced from TRAP staining of 3.6Tpz cells. However, at 8 weeks, H−BMP group showed higher osteoclast activity compared to H+BMP group (Fig. 4, TRAP a&b). Even though the differences in relative radio-opacity were not statistically significant, the transgenic fluorescent reporter model indicates the possible differences in cellular activity at the healing sites. Further studies using longer time points with higher *n* values are required to understand the cellular processes involved in rhBMP-2 mediated bone regeneration and remodeling.

The normal bone repair and regeneration process is complex and requires suitable extracellular matrix scaffold, cells and osteoinductive signals.[35] Previous studies have reported accelerated bone growth in the presence of stem cells alone or in combination with BMPs.[8,36,37] Combining rhBMP-2 with cells may serve as an attractive strategy to reduce rhBMP-2 dose and related side effects, however, the mechanism by which transplanted cells contribute to tissue regeneration in the presence of rhBMP-2 remains poorly understood. Our previous studies comparing calvarial osteoprogenitors (OPCs) and fresh bone marrow cells (fBMCs) showed that the donor cell type can make a significant impact on the extent of bone formation and on the origin of the newly formed bone. Donor-dominated bone regeneration was observed with OPCs, whereas fBMCs promoted host-derived bone formation even though the extent of bone formation was lower than the OPC group.[16]

In the present study, BMSCs enriched via their preferential attachment to tissue culture plastic (plastic adherence method) were used as the donor cells. The microarray analysis of BMSCs showed expression of genes consistent with osteogenic lineage. These BMSCs have shown to promote a donor derived bone regeneration cascade unlike fBMCs.[22] Addition of BMSCs along with rhBMP-2 (H+C+BMP) led to a significant increase in relative radio-opacity of the regenerated tissue when compared to H+BMP group at 4 weeks indicating a synergistic effect ($p = 0.021$). Healos was able to localize the transplanted Cyan cells at the defect site and cells deposited copious amounts of disorganized early woven bone-like matrix at 4 weeks, possibly due to the stimulation of the multipotent donor cells by rhBMP-2. Significant variability in TRAP positive cellular activity observed at 4 weeks is presumably due to the disorganized mineralized matrix resulting in differences in the remodeling process. By 4 weeks, the H+BMP group showed host cell activation and recruitment to the defect site, however, the H+C+BMP group showed fewer host-derived (green) cells even in the presence of 2 μg of rhBMP-2.

The X-ray images confirmed complete closure of the defect site in H+C+BMP group, at both the time points. However, the relative radio-opacity of H+C+BMP group at 4 weeks (1.62 ± 0.34) was greater than that observed at 8 weeks (0.98 ± 0.18), even though the difference was not statistically significant ($p = 0.052$). The histological analysis showed differences between the H+C+BMP groups at 4 and 8 weeks. At 8 weeks, both H+C−BMP and H+C+BMP groups showed a thin cortical-type donor derived bone resembling the diaphysis of long bone with a central marrow cavity. Even though no rhBMP-2 was included in the H+C−BMP group, based on the results of the first study, it is possible that rhBMP-2 implanted in the H+C+BMP side has affected the H+C−BMP side. The remodeled cortical-type bone observed at this time point was derived from Col3.6Cyan cells colocalized with

ALP, indicating minimal host cell participation. The results suggest that when an exogenous cell population having a tendency to undergo osteogenic differentiation, for example, BMSCs, is implanted at the defect site, the donor progenitors play a key role in the formation of regenerated bone even in the presence of rhBMP-2. The host bone—regenerated bone interface, however, showed the presence of both donor and host cells indicating an improved osseointegration at cellular level, in the presence of donor cell population.

Zara et al.[38] showed cyst-like bony shells filled with adipocyte-rich matrix, in a rat femoral segmental defect model at high BMP-2 concentrations (11.25, 22.5, and 45 μg per defect). This has been attributed to BMP-induced adipogenesis through activation of the transcription factor peroxisome proliferator activated receptor gamma (PPARγ), a key regulator of adipocyte commitment. The high-magnification images of the marrow-like matrix at 8 weeks showed structural similarity to normal bone marrow with very few adipocytes, similar to the diaphysis of long bone. Our recent studies have shown that the progenitors derived from neonatal calvaria generate a membranous-like bone and show little trophism for interacting with host-derived progenitor.[22] In contrast, progenitors derived from BMSCs in the present study formed a cortical-like bone structure that is richly invested with bone marrow and which readily integrates with the surrounding bone. The source of the stem cells has been shown to influence the differentiation potential of cells.[39] Our results indicated that the source of the cells may also affect the properties of the regenerated bone, presumably due to the cells retaining the memory of their origin. Further studies are needed to understand the role of cellular memory in determining the properties of the regenerated bone.

CONCLUSIONS

This study provided insights into the cellular processes of bone formation in scenarios where an osteoinductive factor is present alone or with multipotent cells. An important step to improve the clinical outcome of BMP-based treatments would be to control the release of BMP and localize its effect at the site of implantation. The study demonstrated the significant off-target effect of rhBMP2 in the bilateral calvarial defect when delivered using the collagen-hydroxyapatite scaffold. Even though the implantation site and neighboring site showed bone formation by 4 weeks, the bone remodeling cascade was found to be different at the two sites demonstrating the potential differences in cellular activity. Despite the potent cell homing effect of rhBMP-2, the cell transplantation study using fluorescent reporter cells confirmed the inability of rhBMP-2 to recruit host cells in the presence of donor BMSCs. Use of multiple fluorescent protein reporters has the potential to provide a functional read out of the cellular responses toward scaffold/growth factor based bone regeneration strategies.

Supplementary Material

Refer to Web version on PubMed Central for supplementary material.

Acknowledgments

References

1. Verma S, Domb AJ, Kumar N. Nanomaterials for regenerative medicine. Nanomedicine (Lond). 2011; 6:157–181. [PubMed: 21182426]

2. Rodrigues M, Griffith LG, Wells A. Growth factor regulation of proliferation and survival of multipotential stromal cells. Stem Cell Res Ther. 2010; 1:1–12.

3. Deschaseaux F, Sensebe L, Heymann D. Mechanisms of bone repair and regeneration. Trends Mol Med. 2009; 15:417–29. [PubMed: 19740701]

4. Jeon EJ, Lee KY, Choi NS, Lee MH, Kim HN, Jin YH, Ryoo HM, Choi JY, Yoshida M, Nishino N, Oh BC, Lee KS, Lee YH, Bae SC. Bone morphogenetic protein-2 stimulates Runx2 acetylation. J Biol Chem. 2006; 281:16502–16511. [PubMed: 16613856]

5. Jo S, Kim S, Cho TH, Shin E, Hwang SJ, Noh I. Effects of recombinant human bone morphogenic protein-2 and human bone marrow-derived stromal cells on *in vivo* bone regeneration of chitosan–poly(ethylene oxide) hydrogel. J Biomed Mater Res Part A. 2013; 101A:892–901.

6. Stephan SJ, Tholpady SS, Gross B, Petrie-Aronin CE, Botchway EA, Nair LS, Ogle RC, Park SS. Injectable tissue-engineered bone repair of a rat calvarial defect. Laryngoscope. 2010; 120:895–901. [PubMed: 20422682]

7. Kolf CM, Cho E, Tuan RS. Biology of adult mesenchymal stem cells: Regulation of niche, self-renewal and differentiation. Arthritis Res Ther. 2007; 9:204–214. [PubMed: 17316462]

8. Burastero G, Scarfi S, Ferraris C, Fresia C, Sessarego N, Fruscione F, Monetti F, Scarfo F, Schupbach P, Podesta M, Grappiolo G, Zocchi E. The association of human mesenchymal stem cells with BMP-7 improves bone regeneration of critical-size segmental bone defects in athymic rats. Bone. 2010; 47:117–126. [PubMed: 20362702]

9. Li F, Whyte N, Niyibizi C. Differentiating multipotent mesenchymal stromal cells generate factors that exert paracrine activities on exogenous MSCs: Implications for paracrine activities in bone regeneration. Biochem Biophys Res Commun. 2012; 426:475–479. [PubMed: 22960177]

10. Bishop GB, Einhorn TA. Current and future clinical applications of bone morphogenetic proteins in orthopaedic trauma surgery. Int Orthop. 2007; 31:721–727. [PubMed: 17668207]

11. Seeherman H, Wozney JM. Delivery of bone morphogenetic proteins for orthopedic tissue regeneration. Cytokine Growth Factor Rev. 2005; 16:329–345. [PubMed: 15936978]

12. Burks MV, Nair LS. Long-term effects of bone morphogenetic protein based treatments in humans. J Long Term Eff Med Implants. 2010; 20:277–293. [PubMed: 21488821]

13. Kalajzic I, Kalajzic Z, Kaliterna M, Gronowicz G, Clark SH, Lichtler AC, Rowe D. Use of type I collagen green fluorescent protein transgenes to identify subpopulations of cells at different stages of the osteoblast lineage. J Bone Miner Res. 2002; 17:15–25. [PubMed: 11771662]

14. Lee TC, Mohsin S, Taylor D, Parkesh R, Gunnlaugsson T, O'Brien FJ, Giehl M, Gowin W. Detecting microdamage in bone. J Anat. 2003; 203:161–172. [PubMed: 12924817]

15. Liu Y, Wang L, Fatahi R, Kronenberg M, Kalajzic I, Rowe D, Li Y, Maye P. Isolation of murine bone marrow derived mesenchymal stem cells using Twist2 Cre transgenic mice. Bone. 2010; 47:916–925. [PubMed: 20673822]

16. Yu X, Wang L, Peng F, Jiang X, Xia Z, Huang J, Rowe D, Wei M. The effect of fresh bone marrow cells on reconstruction of mouse calvarial defect combined with calvarial osteoprogenitor cells and collagen–apatite scaffold. J Tissue Eng Regen Med. 2013; 7:974–983. [PubMed: 22473786]

17. Jiang X, Kalajzic Z, Maye P, Braut A, Bellizzi J, Mina M, Rowe DW. Histological analysis of GFP expression in murine bone. J Histochem Cytochem. 2005; 53:593–602. [PubMed: 15872052]

18. Ushiku C, Adams DJ, Jiang X, Wang L, Rowe DW. Long bone fracture repair in mice harboring GFP reporters for cells within the osteoblastic lineage. J Orthop Res. 2010; 28:1338–1347. [PubMed: 20839319]

19. Luvizuto ER, Tangl S, Zanoni G, Okamoto T, Sonoda CK, Gruber R, Okamoto R. The effect of BMP-2 on the osteoconductive properties of beta-tricalcium phosphate in rat calvaria defects. Biomaterials. 2011; 32:3855–3861. [PubMed: 21376389]

20. Xiao W, Fu H, Rahaman MN, Liu Y, Bal BS. Hollow hydroxyapatite microspheres: A novel bioactive and osteoconductive carrier for controlled release of bone morphogenetic protein-2 in bone regeneration. Acta Biomater. 2013; 9:8374–8383. [PubMed: 23747325]

21. Schantz JT, Woodruff MA, Lam CX, Lim TC, Machens HG, Teoh SH, Hutmacher DW. Differentiation potential of mesenchymal progenitor cells following transplantation into calvarial defects. J Mech Behav Biomed Mater. 2012; 11:132–142. [PubMed: 22658162]

22. Rowe, D. Improving Soldier Recovery from Catastrophic Bone Injuries: Developing an Animal Model for Standardizing the Bone Reparative Potential of Emerging Progenitor Cell Therapies. Farmington, CT: University of Connecticut; Aug 1. 2011 p. 1-29.Award Number: W81XWH-07-2-0085

23. Viateau, V.; Logeart-Avramoglou, D.; Guillemin, G.; Petite, H. Animal models for bone tissue engineering purposes. In: Conn, PM., editor. Sourcebook of Models for Biomedical Research. Humana Press; Totowa, New Jersey: 2008. p. 725-736.

24. Liu Y, Enggist L, Kuffer AF, Buser D, Hunziker EB. The influence of BMP-2 and its mode of delivery on the osteoconductivity of implant surfaces during the early phase of osseointegration. Biomaterials. 2007; 28:2677–2686. [PubMed: 17321590]

25. Kraiwattanapong C, Boden SD, Louis-Ugbo J, Attallah E, Barnes B, Hutton WC. Comparison of Healos/bone marrow to INFUSE(rhBMP-2/ACS) with a collagen-ceramic sponge bulking agent as graft substitutes for lumbar spine fusion. Spine (Phila Pa 1976). 2005; 30:1001–1007. discussion 1007. [PubMed: 15864149]

26. Freilich M, M Patel C, Wei M, Shafer D, Schleier P, Hortschansky P, Kompali R, Kuhn L. Growth of new bone guided by implants in a murine calvarial model. Bone. 2008; 43:781–788. [PubMed: 18589010]

27. Rahman CV, Ben-David D, Dhillon A, Kuhn G, Gould TWA, Müller R, Rose FRAJ, Shakesheff KM, Livne E. Controlled release of BMP-2 from a sintered polymer scaffold enhances bone repair in a mouse calvarial defect model. J Tissue Eng Regen Med. 2014; 8:59–66. [PubMed: 22678704]

28. Xie G, Sun J, Zhong G, Liu C, Wei J. Hydroxyapatite nanoparticles as a controlled-release carrier of BMP-2: Absorption and release kinetics *in vitro*. J Mater Sci Mater Med. 2010; 21:1875–1880. [PubMed: 20300953]

29. Otsuru S, Tamai K, Yamazaki T, Yoshikawa H, Kaneda Y. Bone marrow-derived osteoblast progenitor cells in circulating blood contribute to ectopic bone formation in mice. Biochem Biophys Res Commun. 2007; 354:453–458. [PubMed: 17239347]

30. Kimura Y, Miyazaki N, Hayashi N, Otsuru S, Tamai K, Kaneda Y, Tabata Y. Controlled release of bone morphogenetic protein-2 enhances recruitment of osteogenic progenitor cells for de novo generation of bone tissue. Tissue Eng Part A. 2010; 16:1263–1270. [PubMed: 19886805]

31. Mariner PD, Wudel JM, Miller DE, Genova EE, Streubel SO, Anseth KS. Synthetic hydrogel scaffold is an effective vehicle for delivery of INFUSE (rhBMP2) to critical-sized calvaria bone defects in rats. J Orthop Res. 2013; 31:401–416. [PubMed: 23070779]

32. Martino MM, Tortelli F, Mochizuki M, Traub S, Ben-David D, Kuhn GA, Muller R, Livne E, Eming SA, Hubbell JA. Engineering the growth factor microenvironment with fibronectin domains to promote wound and bone tissue healing. Sci Transl Med. 2011; 3:100ra89.

33. Cowan CM, Aalami OO, Shi YY, Chou YF, Mari C, Thomas R, Quarto N, Nacamuli RP, Contag CH, Wu B, Longaker MT. Bone morphogenetic protein 2 and retinoic acid accelerate *in vivo* bone formation, osteoclast recruitment, and bone turnover. Tissue Eng. 2005; 11:645–658. [PubMed: 15869441]

34. Kaneko H, Arakawa T, Mano H, Kaneda T, Ogasawara A, Nakagawa M, Toyama Y, Yabe Y, Kumegawa M, Hakeda Y. Direct stimulation of osteoclastic bone resorption by bone morphogenetic protein (BMP)–22 and expression of BMP receptors in mature osteoclasts. Bone. 2000; 27:479–486. [PubMed: 11033442]

35. Ripamonti U, Ramoshebi LN, Matsaba T, Tasker J, Crooks J, Teare J. Bone induction by BMPs/OPs and related family members in primates. J Bone Joint Surg Am. 2001; 83-A(Suppl 1(Pt 2)):S116–S127. [PubMed: 11314789]

36. Akita S, Fukui M, Nakagawa H, Fugi T, Akino K. Cranial bone defect healing is accelerated by mesenchymal stem cells induced by coadministration of bone morphogenetic protein-2 and basic fibroblast growth factor. Wound Repair Regen. 2004; 12:252–259. [PubMed: 15086777]

37. Bruder SP, Kurth AA, Shea M, Hayes WC, Jaiswal N, Kadiyala S. Bone regeneration by implantation of purified, culture-expanded human mesenchymal stem cells. J Orthop Res. 1998; 16:155–162. [PubMed: 9621889]

38. Zara JN, Siu RK, Zhang X, Shen J, Ngo R, Lee M, Li W, Chiang M, Chung J, Kwak J, Wu BM, Ting K, Soo C. High doses of bone morphogenetic protein 2 induce structurally abnormal bone and inflammation *in vivo*. Tissue Eng Part A. 2011; 17:1389–1399. [PubMed: 21247344]

39. Polo JM, Liu S, Figueroa ME, Kulalert W, Eminli S, Tan KY, Apostolou E, Stadtfeld M, Li Y, Shioda T, Natesan S, Wagers AJ, Melnick A, Evans T, Hochedlinger K. Cell type of origin influences the molecular and functional properties of mouse induced pluripotent stem cells. Nature Biotechnol. 2010; 28:848–855. [PubMed: 20644536]
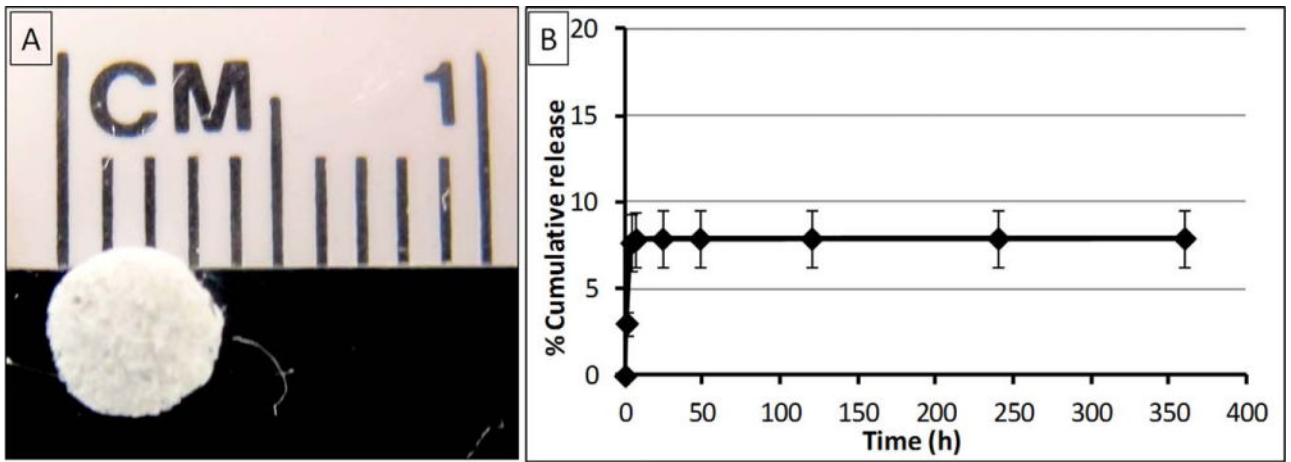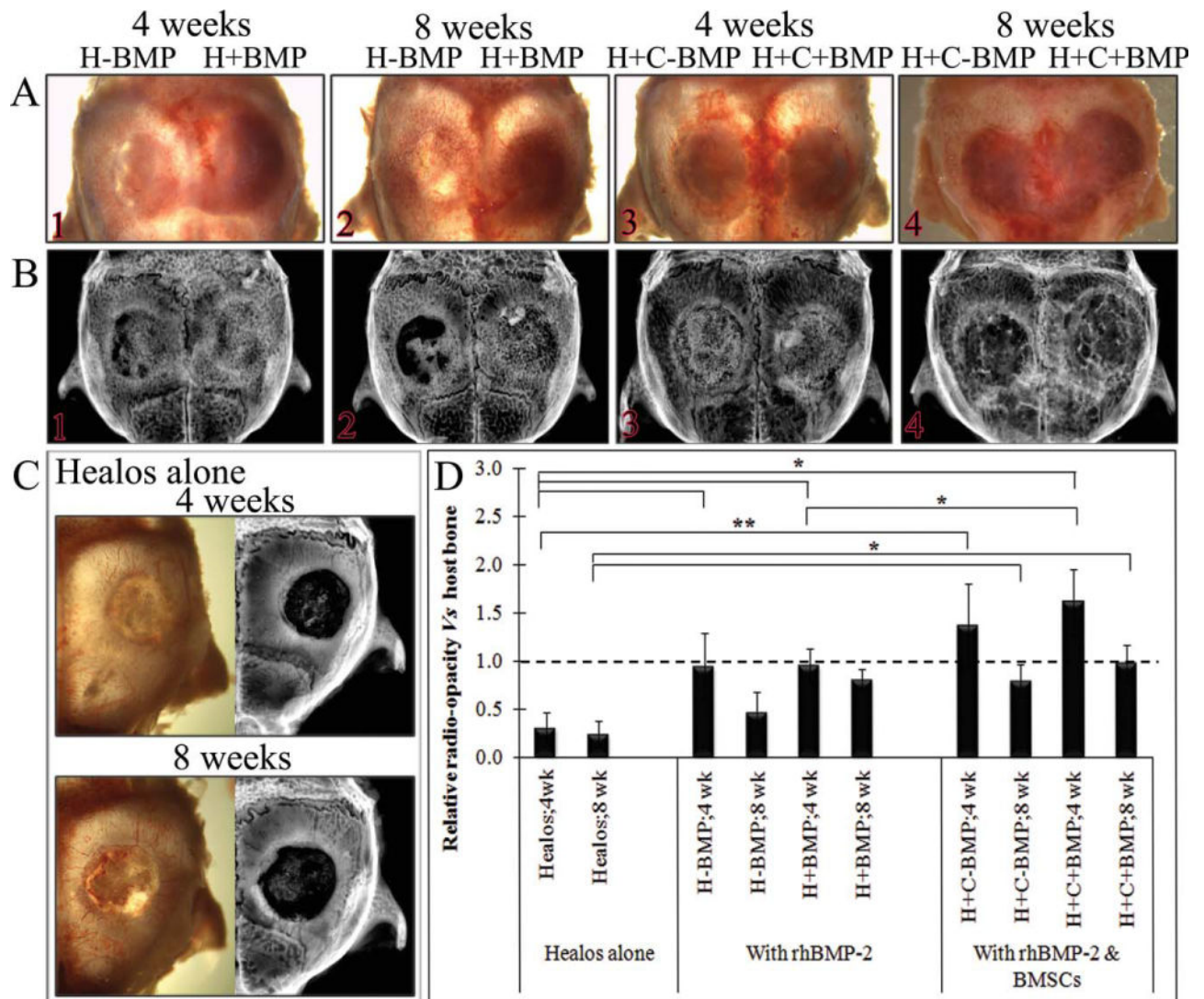
Author Manuscript

Author Manuscript

Author Manuscript

Author Manuscript

FIGURE 1.

A: Healos disc image. B: Cumulative release profile of rhBMP-2 from Healos loaded with 2 μg of rhBMP-2 as a function of time for 15 days. [Color figure can be viewed in the online issue, which is available at wileyonlinelibrary.com.].

FIGURE 2.
Representative images of isolated calvaria showing (A) whole calvaia, (B) X-ray images of the tested groups at 4 and 8 weeks, (C) whole calvaria and X-ray images of Healos alone at 4 and 8 weeks, when neighboring defects did not contain rhBMP-2, and (D) quantification of new bone formation in terms of relative radio-opacity of defect site versus host bone. Statistical analysis was performed using t-test. Data represented as mean ± SD for $n = 3$, *$p < 0.050$; **$p < 0.010$. [Color figure can be viewed in the online issue, which is available at wileyonlinelibrary.com.]
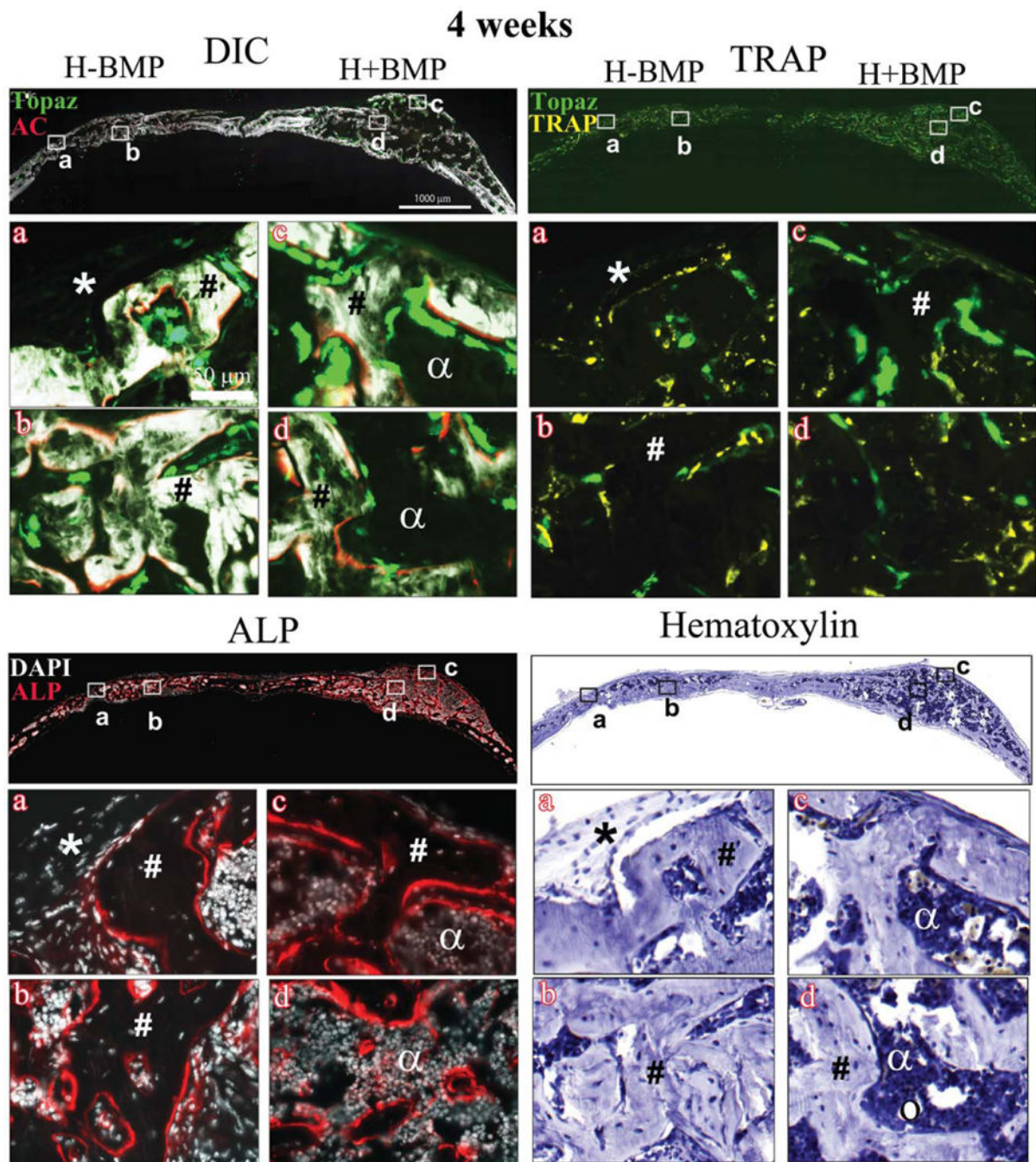
FIGURE 3.

Histology showing DIC-, TRAP-, ALP-, and hematoxylin-stained sections of the critical sized defects after 4 weeks of implantation with Healos with or without rhBMP-2 Full calvarial sections (scale bars: 1000 μm), magnified images a–d (scale bar: 50 μm). DIC sections show activity of GFP reporters in the regenerated tissues colocalized with alizarin complexone (AC). Bright green cells lined with a red mineralizing AC label are mature osteoblasts. Light green elongated cells form a periosteum-like layer at the periphery of the defects. TRAP: Bright yellow stain colocalized with light green cells represents TRAP

positive host-derived osteoclasts. ALP: Red color indicates ALP positive cells. Cell nuclei are stained white with DAPI. (*) Host-derived fibroblastic periosteum-like layer; (#) trabecular-like bone with embedded osteocytes; (α) marrow-like matrix; and (circle) adipocytes. [Color figure can be viewed in the online issue, which is available at wileyonlinelibrary.com.]
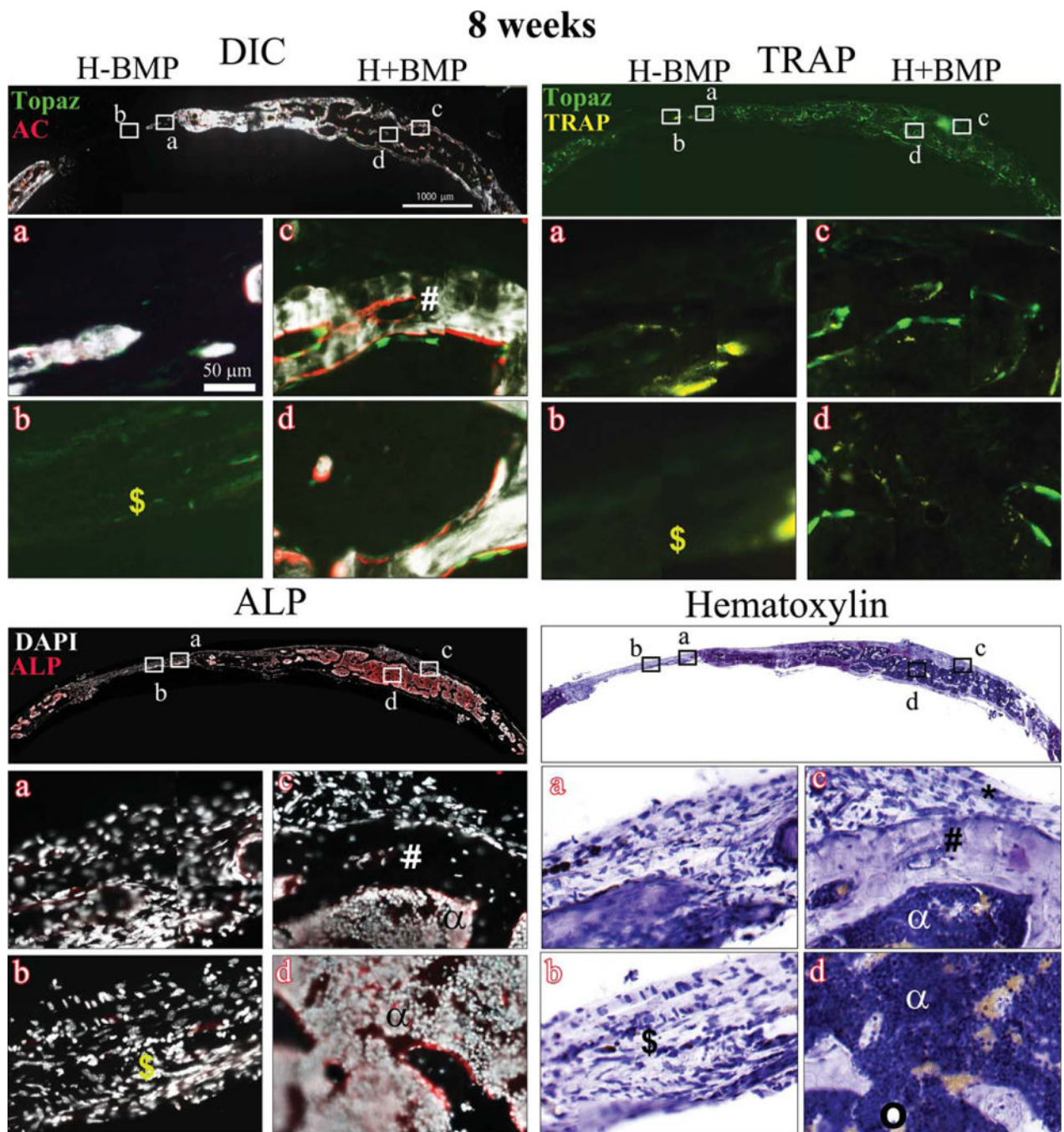
FIGURE 4.

Histology showing DIC-, TRAP-, ALP-, and hematoxylin-stained sections of the critical sized defects after 8 weeks of implantation with Healos with or without rhBMP-2 Full calvarial sections (scale bars: 1000 μm), magnified images a–d (scale bar: 50 μm). DIC sections show activity of GFP reporters in the regenerated tissues colocalized with alizarin complexone (AC). Bright green cells lined with a red mineralizing AC label are mature osteoblasts. Light green elongated cells form a periosteum-like layer at the periphery of the defects. TRAP: Bright yellow stain colocalized with light green cells represents TRAP

positive host-derived osteoclasts. ALP: Red color indicates ALP positive cells. Cell nuclei are stained white with DAPI. (*) Host-derived fibroblastic periosteum-like layer; (#) trabecular-like bone with embedded osteocytes; (α) marrow-like matrix; (circle) adipocytes; and ($) fibrous tissue. [Color figure can be viewed in the online issue, which is available at wileyonlinelibrary.com.]
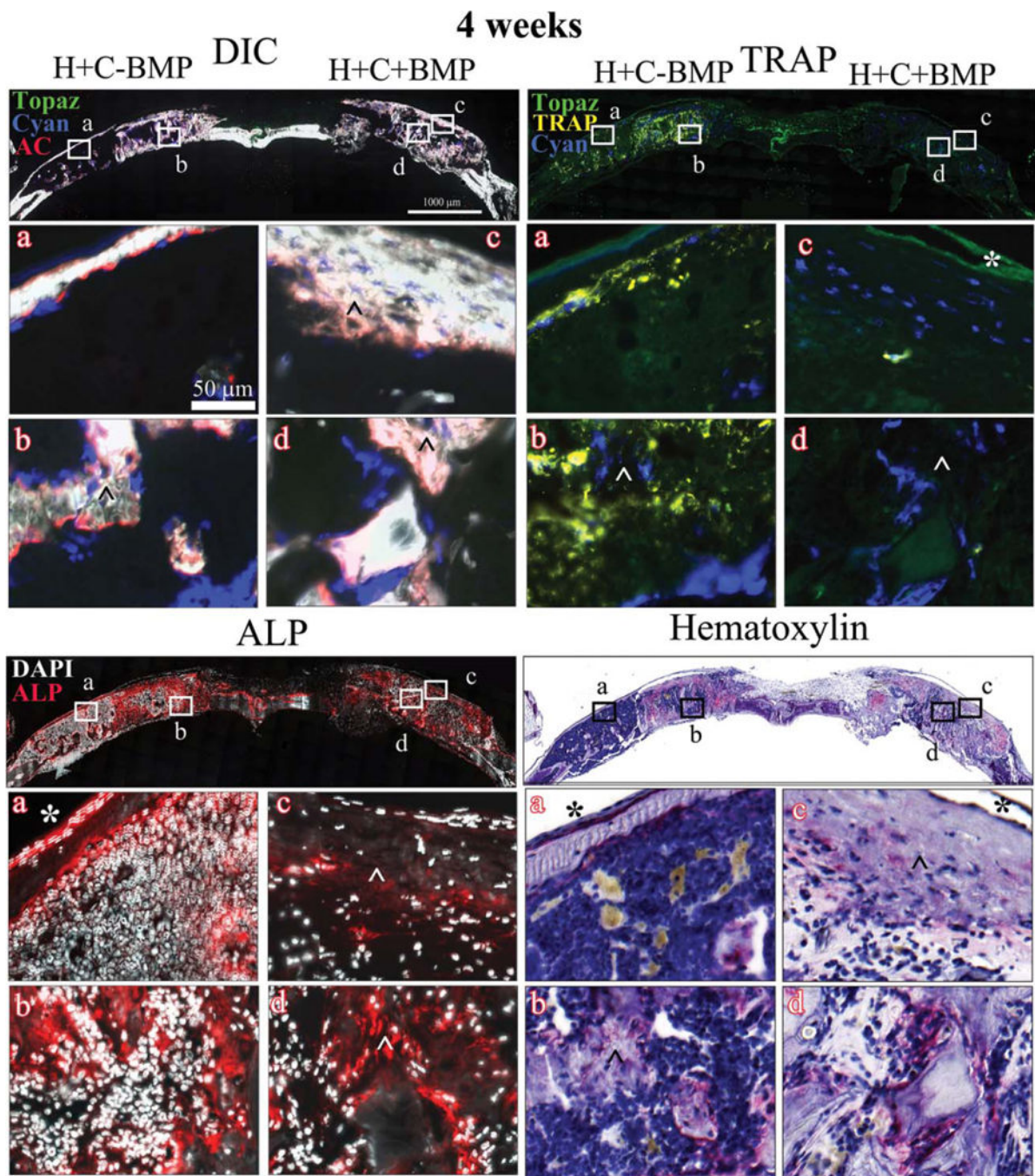
FIGURE 5.

Histology showing DIC-, TRAP-, ALP-, and hematoxylin-stained sections of the critical sized defects after 4 weeks of implantation with Healos along with BMSCs, with or without rhBMP-2 Full calvarial sections (scale bars: 1000 μm), magnified images a–d (scale bar: 50 μm). DIC sections show activity of GFP reporters in the regenerated tissues colocalized with alizarin complexone (AC). Bright green host-derived cells as well as very few donor cell derived bright blue cells are observed, lined with a red mineralizing AC label. These are mature osteoblasts. Host-derived light green elongated cells form a periosteum-like layer is

seen at the periphery of the defects. TRAP: Bright yellow stain colocalized with light green/blue cells represents TRAP positive osteoclasts. ALP: Red color indicates ALP positive cells. Cell nuclei are stained white with DAPI. (^) Early woven bone with disorganized mineralized, ALP positive matrix; (*) host-derived fibroblastic periosteum-like layer.
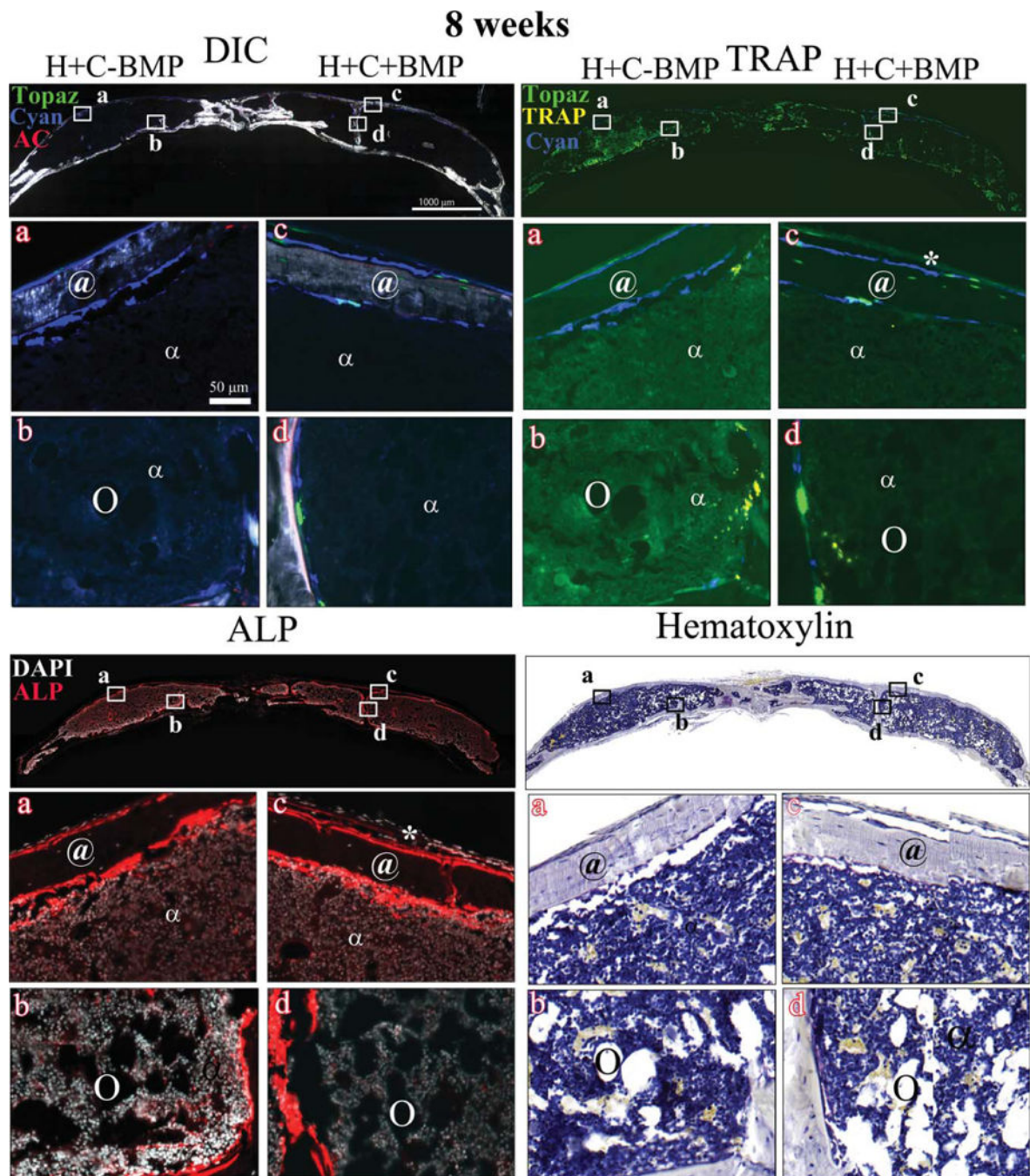
FIGURE 6.

Histology showing DIC-, TRAP-, ALP- and hematoxylin-stained sections of the critical sized defects after 8 weeks of implantation with Healos along with BMSCs, with or without rhBMP-2 Full calvarial sections (scale bars: 1000 µm), magnified images a–d (scale bar: 50 µm). DIC sections show activity of GFP reporters in the regenerated tissues colocalized with alizarin complexone (AC). Mostly donor cell derived bright blue cells with very few bright green host-derived cells are observed, lined with a red mineralizing AC label. These are mature osteoblasts. Host-derived light green elongated cells form a periosteum-like layer is

seen at the periphery of the defects. TRAP: Bright yellow stain colocalized with light green/blue cells represents TRAP positive osteoclasts. ALP: Red color indicates ALP positive cells. Cell nuclei are stained white with DAPI. (*) Host-derived fibroblastic periosteum-like layer; (@) cortical-type bone with embedded osteocytes; (α) marrow-like matrix; and (circle) adipocytes. [Color figure can be viewed in the online issue, which is available at wileyonlinelibrary.com.]

TABLE I

Study Design

Time Point (weeks)	Defect Side[a]	Treatment		Treatment Code
		BMSCs	BMP-2	
4	Right	−	+	H+BMP
	Left	−	−	H−BMP
8	Right	−	+	H+BMP
	Left	−	−	H−BMP
4	Right	+	+	H+C+BMP
	Left	+	−	H+C−BMP
8	Right	+	+	H+C+BMP
	Left	+	−	H+C−BMP

[a]Direction of the defects has been defined with respect to the reader for easier interpretation.

No. of BMSCs implanted: 1×10^6 per defect.

Amount of BMP implanted: 2 μg per defect.